

# DEVELOPMENT OF AN AIRBORNE REMOTE SENSING SYSTEM FOR CROP PEST MANAGEMENT: SYSTEM INTEGRATION AND VERIFICATION

Y. Lan, Y. Huang, D. E. Martin, W. C. Hoffmann

**ABSTRACT.** Remote sensing is being used with Global Positioning Systems, Geographic Information Systems, and variable rate technology to ultimately help farmers maximize the economic and environmental benefits of crop pest management through precision agriculture. Airborne remote sensing is flexible and versatile because fields can be flown at variable altitude depending on the spatial resolution required. Although the use of airborne hyperspectral remote sensing in agricultural research and applications has been steadily increasing in the last decade, the airborne multispectral technique is still a good source of crop, soil, or ground cover information. The MS-4100 is a multispectral camera that produces and aligns images from different bands with a built-in prism. Data can be analyzed from the composite image or individual band images. The camera system evaluated herein uses a camera control system to physically compensate for roll, pitch, and yaw and maintain the camera at vertical nadir orientation. This article describes the automated airborne multi-spectral imaging system and image processing using sample imagery to demonstrate the capability and potential of the system for crop pest management.

**Keywords.** Airborne multi-spectral imaging, Multi-spectral camera, Camera control, Pest management.

Scientists and engineers have developed remote sensing technology along with Global Positioning Systems (GPS), Geographic Information Systems (GIS), and variable rate technology (VRT) to assist farmers in maximizing the economic and environmental benefits of crop pest management in precision agriculture. Image-based remote sensing has been conducted by satellites, aircraft, or ground-based platforms. Satellite remote sensing is appropriate for large-scale studies but often can not meet the spatial resolution requirement of many applications. Ground-based platforms such as handheld spectroradiometers, are typically used for ground truth measurements. Multi-spectral and hyper-spectral imaging systems also are used on ground-based platforms, but slow travel speeds preclude practical use of these systems for anything but small plots or fields. Airborne remote sensing is flexible, has the capability of rapid image acquisition, and is able to achieve varying spa-

tial resolutions at different flight altitudes for the optimal trade-off of resolution and speed of image acquisition.

In airborne remote sensing for agricultural research and applications the use of hyper-spectral sensors has been steadily increasing in the last decade (Willis et al., 1998; Yang et al., 2002, 2004, 2007; Jang et al., 2005). Even so, the airborne multi-spectral technique is still a good source of crop, soil, or ground cover information if principal bands and vegetation indices are carefully chosen to amplify the field feature of interest. Multi-spectral systems are much less expensive and data intensive compared with hyper-spectral systems. So, they are a cost-effective option in many cases.

In pest management, detection of insect damage to crops, weed infestation, and disease provides valuable information for management planning and decision-making. Airborne remote sensing has been used in detection and analysis of pest damage to fields (Everitt and Davis, 2004). Research has been conducted using ground and aerial remote sensing for detection and discrimination of weeds (Gumz and Weller, 2006). There has been a shift away from uniform, early season weed control toward using herbicide-ready crops and the application of post-emergence herbicide only as needed. This strategy change has generated increased interest in using remote sensing to define the extent of weed patches within fields so they can be targeted with variable-rate ground and aerial spray rigs (Pinter et al., 2003). In early work, Richardson et al. (1985) demonstrated that multi-spectral aerial video images could be used to distinguish uniform plots of Johnsongrass and pigweed from sorghum, cotton, and cantaloupe plots. By comparing visual assessment of herbicide injury in cotton with CIR (Color-Infrared) photography, Near-Infrared (NIR) videography, and a wideband handheld radiometer, Hickman et al. (1991) concluded that remote sensing and mapping of moderate herbicide damage was not only possible, but that the application rate of

---

Submitted for review in February 2008 as manuscript number IET 7405; approved for publication by the Information & Electrical Technologies Division of ASABE in May 2009.

Mention of trademark, vendor, or proprietary product does not constitute a guarantee or warranty of the product by the USDA and does not imply its approval to the exclusion of other products that may also be suitable.

The authors are **Yubin Lan, ASABE Life Member Engineer**, Agricultural Engineer, USDA-ARS, Aerial Application Technology, Areawide Pest Management Research Unit, College Station, Texas; **Yanbo Huang, ASABE Member Engineer**, Agricultural Engineer, USDA-ARS, Application and Production Research Unit, Stoneville, Mississippi; **Daniel E. Martin, ASABE Member Engineer**, Agricultural Engineer, and **Wesley C. Hoffmann, ASABE Member Engineer**, Agricultural Engineer, USDA-ARS, Aerial Application Technology, Areawide Pest Management Research Unit, College Station, Texas. **Corresponding author:** Yubin Lan, USDA-ARS, 2771 F&B Road, College Station, TX 77845; phone: 979-260-3759; fax: 979-260-9386; e-mail: ylan@sparc.usda.gov.

herbicides could be estimated. Medlin et al. (2000) evaluated the accuracy of classified airborne CIR imagery for detecting weed infestation levels during early-season Glycine max production. Thomson et al. (2005) evaluated a field imaging system on agricultural aircraft using low-cost digital video to distinguish broadleaf weeds from cotton in the field. Ye et al. (2007) used airborne multi-spectral imagery to discriminate and map weed infestations in a citrus orchard. There have been a number of successful applications of airborne remote sensing in detecting insect infestations for pest management. Hart and Myers (1968) used aerial CIR photography to detect insect infestation on trees in a number of citrus orchards. Aerial CIR film and multi-spectral videography also have been used to detect citrus blackfly and brown soft scale problems in citrus as well as whitefly infestations in cotton (Hart et al., 1973; Everitt et al., 1991, 1994, 1996). Willers et al. (2005) presented site-specific approaches to cotton insect control by developing sampling and airborne remote sensing analysis techniques. Airborne remote sensing technology also has been employed for detecting crop disease and assessing its impact on productivity (Heald et al., 1972; Schneider and Safir, 1975; Henneberry et al., 1979; Cook et al., 1999; Qin et al., 2003; Yang et al., 2005; Franke and Menz, 2007).

For agricultural applications, most airborne multi-spectral imaging systems have used either video or single-band cameras that each represents a single waveband. The still camera systems were typically built with several still cameras lined up together and each of the cameras with a specific filter lens imaging in a specific band, such as blue band, green band, red band, NIR band, and even thermal band (Yang et al., 2000; Dabrowska-Zielinska et al., 2001; Fletcher and Everitt, 2007). This arrangement typically had the problem of misalignment of images representing the different bands. Multi-spectral cameras have been developed that produce and line up the images from the different bands with built-in devices and filters; the data can be analyzed on the composite image or the image from an individual band. The MS-4100 (Geospatial Systems, Inc., West Henrietta, N.Y.) is such a multi-spectral camera. For practical use on aircraft, however, operation of the camera would require a technician to control imaging and any ancillary control functions. This is somewhat impractical for small airplanes (e.g. agricultural), as the pilot cannot perform many functions and fly the airplane simultaneously. Control automation is necessary for the multi-spectral camera system in order to reduce labor required and maintain consistency of system operation. Based on the needs in agricultural research and applications, a camera control system, TerraHawk (TerraVerde Technologies, Inc., Stillwater, Okla.) was evaluated to automate the operation of the MS-4100 multi-spectral camera and to control roll, pitch, and yaw camera stabilization during the flight.

The objectives of this research were: 1) to evaluate the automated airborne multi-spectral imaging system with the integration of the MS-4100 camera and the camera control system, and 2) to demonstrate image processing with sample imagery to present the capability and potential of the system for crop pest management.

## MATERIALS AND METHODS

### MS-4100 MULTI-SPECTRAL CAMERA

The MS-4100 is currently a Geospatial Systems, Inc. product. It is a multi-spectral HDTV (High Definition Television) format 3-CCD (Charge-Coupled Device) color/CIR digital camera. This camera is a straight upgrade of the previously named Duncantech MS-3100 and 2100 cameras. The MS-4100 high-resolution 3-CCD camera provides the ultimate in digital imaging quality with 1920 (horizontal) × 1080 (vertical) pixel array per sensor and wide field of view of 60 degrees with 14-mm, f/2.8 lens. Color-separating optics work in concert with large-format progressive scan CCD sensors to maximize resolution, dynamic range, and field of view. The MS-4100 is available in two spectral configurations: RGB (Red Green Blue) for high quality color imaging and CIR for multi-spectral applications. It images the four spectral bands from 400 to 1000 nm. It acquires separate red (660 nm with 40-nm bandwidth), green (540 nm with 40-nm bandwidth), and blue (460 nm with 45-nm bandwidth) image planes and provides composite color images and individual color plane images. It also acquires and provides composite and individual plane images from red, green, and NIR (800 nm with 65-nm bandwidth) bands that approximate Landsat satellite bands (NASA, Washington, D.C.; USGS, Reston, Va.). The MS-4100 is able to further provide RGB and CIR images at the same time and other custom spectral configurations (table 1). Note that if running the RGB or CIR configuration individually, a base configuration will support any three-tap configuration running at 8 bits per color plane (i.e. 24-bit RGB). Adding a fourth 8-bit tap or outputting 10 bits per color plane will require the additional use of port with a second cable.

The MS-4100 camera configures the digital output of image data with CameraLink standard or parallel digital data in either EIA-644 or RS-422 differential format. The MS-4100 camera works with the NI IMAQ PCI-1424/1428 framegrabber (National Instruments, Austin, Tex.). With the software DTControl-FG (Geospatial Systems, Inc) and the CameraLink configuration, the camera system acquires images from the framegrabber directly from within the DTControl program.

### CAMERA CONTROL SYSTEM

Image acquisition of the MS-4100 camera occurs in four different modes. Three of the modes require an external trigger signal to initiate a new acquisition. Free run mode requires no external control signals and provides high frame rates by overlapping the readout time with the exposure time. In this mode, a technician can directly operate the camera

**Table 1. MS-4100 spectral configurations.**

RGB	Red (660 nm with 40-nm bandwidth), Green (540 nm with 40-nm bandwidth), and Blue (460 nm with 45-nm bandwidth) - color imaging
CIR	Red (660 nm with 40-nm bandwidth), Green (540 nm with 40-nm bandwidth), and NIR (800 nm with 65-nm bandwidth) - color infrared imaging
RGB/CIR	RGB and CIR in a single camera
Multi-spectral	Custom spectral configuration to customer specifications

through the DTControl software on the aircraft. However, this manual operation can cause problems with lack of control of roll, pitch, and yaw camera stabilization during the flight. In order to reduce the labor and maintain the consistency of the image acquisition operation, stabilization control is necessary for the camera system. For the purpose, a TerraHawk camera control system was evaluated for aerial imaging using the MS-4100 multi-spectral camera for integration of camera control computer and software, GIS-based flight navigation software, and GPS-based camera triggering for camera automation and automatic control of roll, pitch, and yaw camera stabilization during flight (fig. 1).

As a component of the camera control system, a gimbal is provided for camera mounting for autonomous compensation of roll, pitch, and yaw. The gimbal maintains camera position at or near vertical nadir view and corrects for aircraft yaw by aligning the camera with the GPS heading. The camera is mounted in the gimbal by use of a secure, adjustable height lock. Vertical positioning allows optimal placement of the camera within the fuselage port, even placing the camera several inches below the gimbal if needed. The gimbal axis is located near the base to minimize side to side displacement of the camera due to the gimbal operation when the camera is placed in the camera control system. After use, the camera can be detached from the gimbal for protected storage.

As another component of the camera control system, a (8.4-in., 2.1-lb) touch pad was provided to interface the system control computer. The computer uses a small industrial motherboard. It was selected primarily for its small size, low power requirement, and its PCI slot interface. An onboard PCI slot is required for the most advantageous use of the NI IMAQ 1424/1428 board. The fastest processor available is used for this board configuration, 512MB of memory, and a 20-GB mobile hard drive for data transfer between the camera control system and desktop computers. The touch pad is a sunlight readable LCD display that can be strapped to the pilot's leg as a knee board. It offers a resolution of  $800 \times 600$  and allows user input by either a

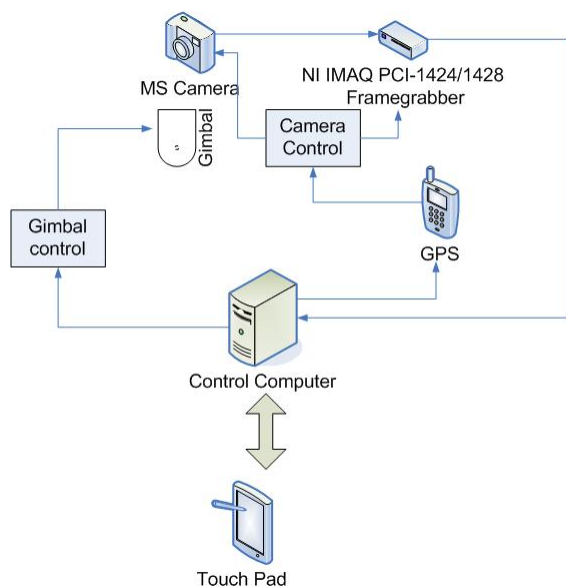


Figure 1. MS-4100 camera control system structure.

touch screen or a stylus pen. Actually, during flight, the pilot does not have to use the touch pad. The pad is primarily used when setting up the imaging mission. This would include uploading field shape files and downloading the images from the system after flight. The imaging mission can be set up prior to flight so that the pilot can concentrate on safe operation of the airplane. However, when multiple fields must be imaged, some operator input is necessary to change the view and guidance to the target field. From a safety standpoint, if multiple fields need to be imaged, it is best to have someone other than the pilot operate the TerraHawk.

With the gimbal, MS-4100 camera, control computer, touch pad, and system integration box containing a GPS unit, the camera control system was assembled (fig. 2). The box of the camera control system was placed over a 38-cm diameter opening in the rear cargo area of a single engine aircraft Cessna U206 (Cessna Aircraft Company, Wichita, Kans.). Navigation and control software was used to operate the camera control system. The software displays a moving map that gives the current aircraft location relative to the fields that need to be imaged. It automates image acquisition by automatically triggering the camera to start imaging at a preset interval once the plane crosses the field boundary. Images also can be taken at any time by pressing a manual image button. The field boundaries are defined by ESRI shape files, which are selected during the flight setup. A GPS track also can be displayed and saved showing the path the plane flew for future reference. The software also manages file directories, and transfers files to the removable device for post-flight data retrieval when exiting the software. Besides in-flight navigation and control, the software supports in-flight imaging simulation as well. During the flight, the camera is triggered by GPS location. The auto control feature optimizes camera exposure settings.

#### IRRADIANCE SENSOR

In order to compare the images acquired at different times, digital numbers (DNs) representing relative pixel intensity need to be normalized to percent reflectance. For the normalization, a radiometer is used to record solar irradiance. The IRR 180 irradiance radiometer (TerraVerde Technologies, Inc., Stillwater, Okla.) is equipped to record the Sun's irradiance in the field to normalize images. This radiometer is set in the field on the test day and automatically records



Figure 2. Complete camera control system assembly.

at a preset interval. After the test, the data are uploaded to the computer. The dedicated image correction software, Image Correction Center software (TerraVerde Technologies, Inc., Stillwater, Okla.), will filter out anomalies caused by clouds and normalize images. Compared with using ground-based reference targets, using the irradiance radiometer makes the image normalization rapid and automatic.

The procedure of image normalization with the IRR 180 irradiance radiometer was developed based on the Schiebe method (<http://www.terraverdetech.com/SchiebeMethod/index.php>) for the use of radiometers and instrument calibration to provide an efficient and practical means to acquire reflectance images without the conventional standard reflectance panels. Basically, this method first converts the digital numbers (DN) of the raw images to the radiance images based on the camera calibration. In order to complete the transformation to reflectance it is necessary to quantify solar irradiance at the time the image was acquired. This is accomplished by radiometers designed for this purpose. Merging radiance images and solar irradiance data is the final step to calculate true reflectance images. The relationship is pixel radiance divided by solar irradiance illuminating the target ( $\Pi = 3.1416$ ):

$$\text{Reflectance} = \Pi * \text{Radiance} / \text{Irradiance} \quad (1)$$

When merging radiance images and solar irradiance data, the image correction software performs this reflectance calculation and generates the corresponding reflectance images.

#### AIRBORNE IMAGE ACQUISITION AND PROCESSING

The hardware and software of the airborne multi-spectral imaging system were integrated, installed and configured on the Cessna U206. The Image Correction Center software (TerraVerde Technologies, Inc., Stillwater, Okla.) and ERDAS Imagine (Leica Geosystems Geospatial Imaging, Atlanta, Ga.) remote sensing image analysis and correction software were installed on a separate desktop computer for radiometric and geometric corrections, respectively, for the images acquired by the airborne multi-spectral imaging system. ArcGIS was installed on the desktop computer to provide the shape files of the fields and to interact with ERDAS Imagine for visualization of image results. A GPS unit, MobileMapper CE (MMCE) (Thales Navigation, Inc., Santa Clara, Calif.), was used to record and map ground control points (GCP) in the fields to establish the spatial distribution of the ground truth measurement.

## RESULTS AND DISCUSSION

The camera control system was operated on the Cessna U206 to image a number of fields for pest management research starting in March, 2007. The purpose of the research was to determine whether the system was able to identify any pest issues in the fields concerned. Because of limited space, the images of one field will be presented and explained. Georectification errors from image obtained using flight-dynamics compensation are also compared with a digital image that was not dynamically compensated in-flight.

The field used for this study was located in the eastern part of Burleson County, Texas (fig. 3). The field had a rotation of corn and cotton each year. In 2007, cotton was planted, and

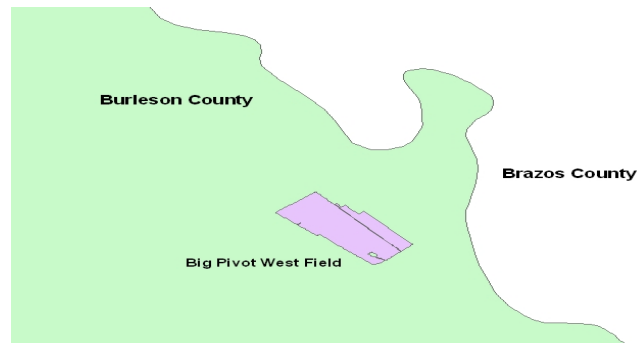


Figure 3. GIS polygon map of the big pivot west field.

in September the field was ready for harvest. Before harvesting the field, defoliant was applied to facilitate harvesting.

In order to implement schemes of site-specific application, an overall map of the field was needed before application of defoliant to provide a prescription for variable-rate application. The map was to reveal the spatial distribution of the cotton growth over the vegetated field and to identify the pest issues over the field for future farming.

Figure 4 shows the CIR image of the field on 20 September, and this image was converted to the reflectance image using the image correction software with the measurement of the irradiance radiometer the same day.

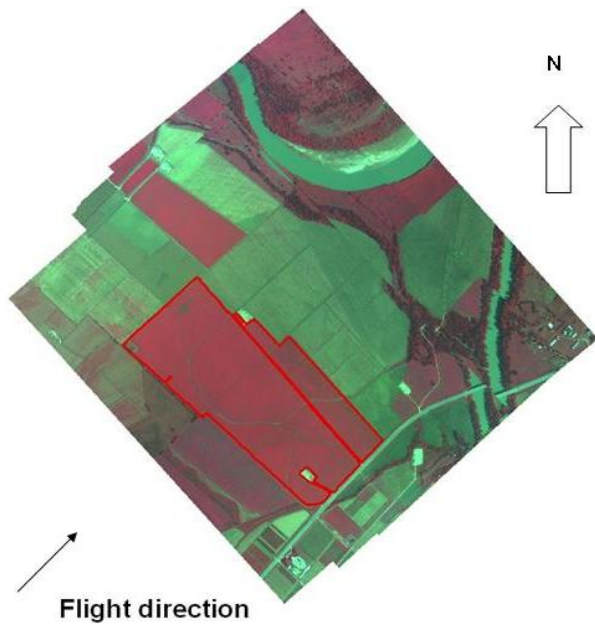
The Cessna U206 carrying the integrated airborne multi-spectral imaging system flew over the field producing the image series over the two enclosed field polygons (fig. 5). The first image in the series covers the field perfectly by visual observation. It was chosen for further processing and analysis.

As an important step of image processing, geometric correction was conducted to reduce geometric distortion of the image and to georeference the image. For geometric correction, the four GCPs were collected and used, and the image was resampled to match the World Geodetic System (WGS) 84 (Department of Defense, Washington, D.C.) with a RMS (Root Mean Square Error) less than half of the image pixel size. This is a good rule of thumb to the geographic location and orientation of the field (fig. 6) because the perfect transformation with an RMS error of 0 is unrealistic. Table 2 illustrates the RMS values of seven georeferenced images acquired using the camera control system with automatic control of roll, pitch, and yaw camera stabilization during the flights for this research. With the flight altitude of 2600 m, the image resolution was 1.56 m/pixel for the MS-4100 camera. All of the RMS values in table 2 are much



Figure 4. An image of the cotton field on 20 September 2007.





**Legend**

Field Polygon Boundary 1:890,000

Figure 5. Image series on 20 September 2007.

less than the calculated  $1.56/2 = 0.753$  m. However, when the digital camera was used during flight without the camera automated control, image georeferencing was a challenge. Figure 7 illustrates an RGB digital image taken by the Sony DSC (Digital Still Camera) F828 (Sony Corporation, Tokyo, Japan) at a flight altitude of 2100 m. The georeferenced image also is illustrated. Although the pilot attempted to fly straight, the camera position was off the vertical nadir view of the field without the camera control compensation. With the 28-mm lens and flight altitude, image pixel resolution was 0.53 m/pixel while the minimal RMS of image

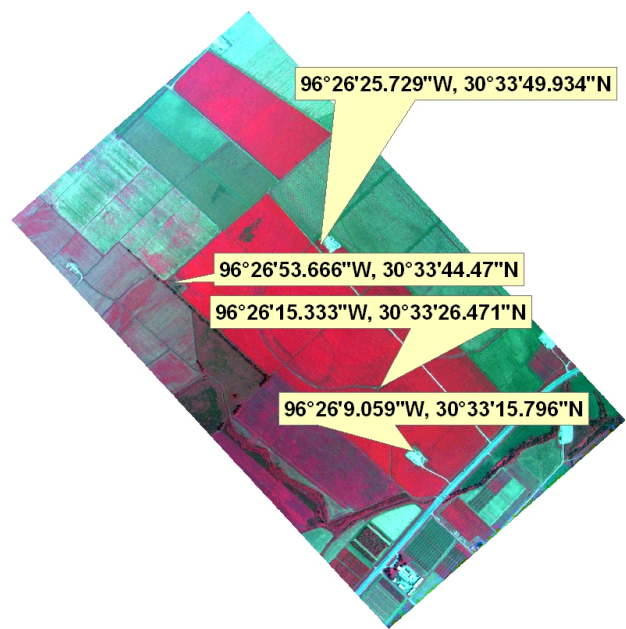


Figure 6. GCPs and geometrically corrected image on 20 September 2007.

**Table 2. RMS values of seven georeferenced images acquired using the camera control system.<sup>[a]</sup>**

Image Date	RMS (m)
20 August 2007	0.2445
14 September 2007	0.2580
20 September 2007	0.2631
27 September 2007	0.1517
2 October 2007	0.1542
5 October 2007	0.1794
11 October 2007	0.2134

[a] Images were obtained at 2600-m altitude (1.56 m/pixel resolution).

**Mismatches between field boundary and GIS polygon of the field**



Figure 7. RGB digital image and georeferenced image with overlay of GIS polygon of the big pivot west field.

georeference using the same four GCPs as figure 6 was 0.33 m. This result was unacceptable as it is greater than  $0.53/2 = 0.27$  m. The georeferenced RGB digital image in figure 7 presents some mismatches between the field boundary and the GIS polygon while figure 6 shows a near-perfect match between them on the CIR image. This indicates that the utility of the camera control system in compensating images for changing flight dynamics.

After geometric correction using ERDAS, the image was cropped to the area of interest (AOI) to focus on the field concerned (fig. 8). By going over the image it was found that the field presented a pattern of center pivot irrigation, intersecting dirt roads, ditches, and varied vegetation of canopy mainly due to spatial change of soil profile over the field. The image also showed that two regions within the crop canopy in the field indicated different spectral signatures from the surrounding area. By ground truth field inspection, it was discovered that a number of abandoned irrigation structures remained in Region A. Region B was infested with cotton root rot disease (fig. 9).

Root rot is a common pest issue in cotton growth. Identification of the region of cotton root rot and detection of the change of this pest issue are important for current and future farming of the field. For the purpose of identification and detection, the image was further cropped into a much smaller CIR AOI to focus on the region of cotton root rot (fig. 10). The image AOI was evaluated by individual bands, and we found that the images of NIR and red bands indicated the existence of root rot regions. The green band showed mostly noise and did not present visual differences (fig. 10). It appears by subjective evaluation of figure 10 that the NIR and red images and possible band combinations such as NIR/red ratio and NDVI (Normalized Difference Vegetation Index) are probably sufficient to identify the region of root rot infestation (Yang et al., 2003).

In order to detect the change of the root rot infested region, the temporal analysis should be incorporated. Figure 11 shows the NIR images of the root rot infested region on 20 August, 14 September, 20 September, 27 September,



Figure 9. Root rot of cotton crop.

2 October, 5 October, and 11 October of 2007. The images on 20 August, 14 September, 20 September, and 27 September showed the infested regions clearly, and on subsequent days, the images showed infestation clearly even after the defoliant was applied on 28 September 2007. Therefore, all

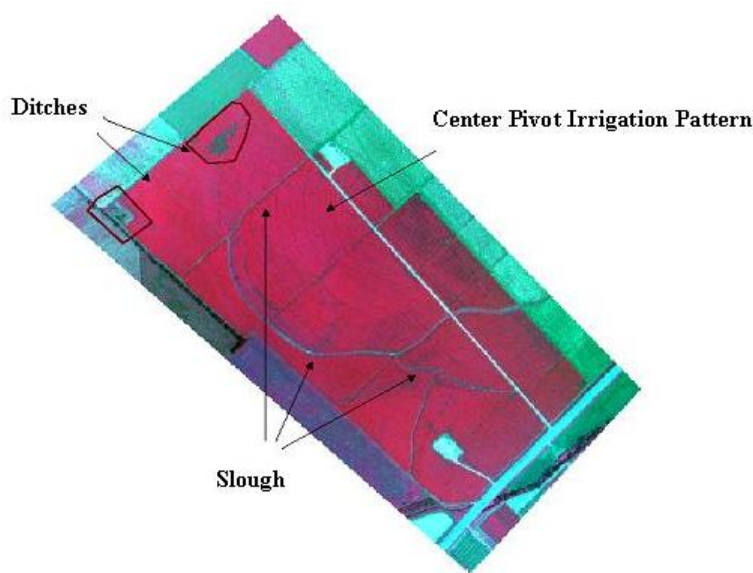


Figure 8. AOI of the processed image and features of the field demonstrated on the image on 20 September 2007.



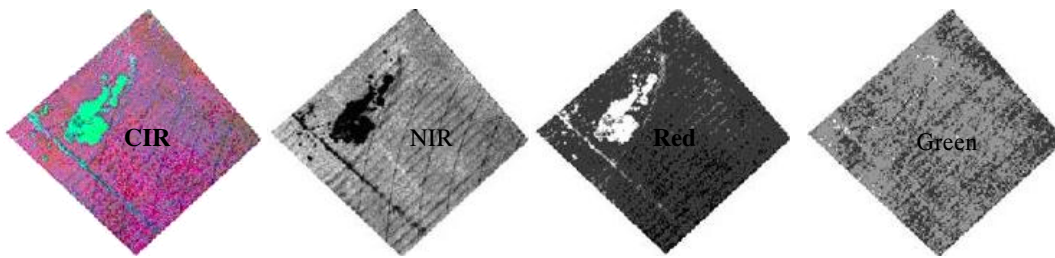


Figure 10. CIR AOI and individual band AOI images.

images were good data sources to quantify the temporal change of root rot infestation in the region. However, care should be taken when examining the difference between images before and after defoliant application.

For variable rate application of defoliant over the field, a prescription map would be required. To produce the prescription map, data revealing the spatially varying distribution of the cotton canopy is required. A number of options are available to provide the data. An NDVI map is one option. Figure 12 is the NDVI map of the field, in which the bright pixels represent high-vigor vegetation points and the dark pixels represent low-vigor vegetation points.

## CONCLUSIONS

The integration of a MS-4100 multi-spectral camera with a specifically designed camera control system described in this article has great potential to be a cost-effective tool of airborne remote sensing in pest management. The automated multi-spectral imaging system is able to consistently produce images at or near vertical nadir view for the spatial, spectral, and temporal analysis of pest issues. Example imagery showed the utility of the flight dynamics control system in reducing spatial errors caused by airplane roll, tilt, and yaw. Depending on the spatial errors that can be tolerated

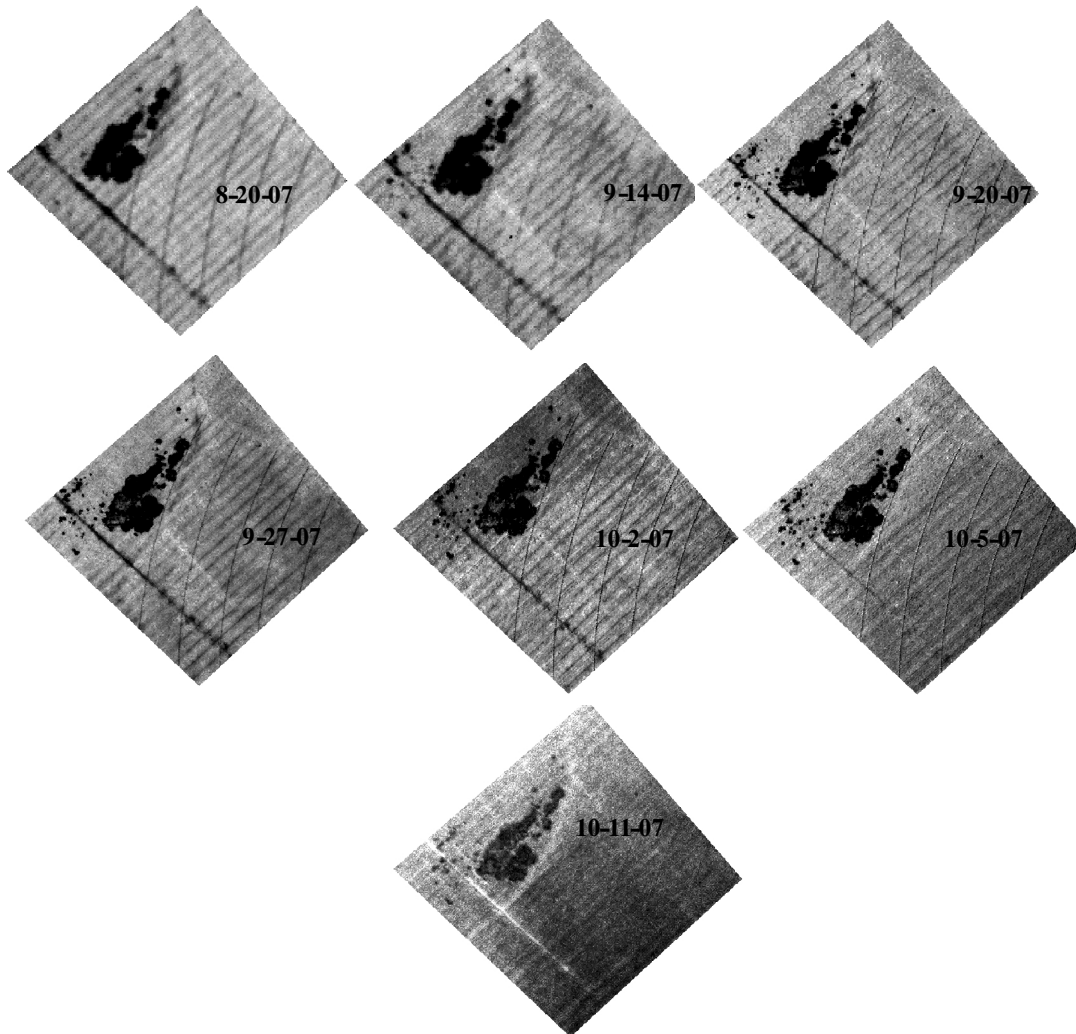


Figure 11. NIR images of the root rot infested region on different dates.



Figure 12. NDVI image of the field on 20 September 2007.

for any given application, further georectification post-processing may or may not be required.

#### ACKNOWLEDGEMENTS

Special thanks to Mr. Lee Denham for his help in making the successful flights for image acquisition.

#### REFERENCES

Cook, C. G., D. E. Escobar, J. H. Everitt, I. Cavazos, A. F. Robinson, and M. R. Davis. 1999. Utilizing airborne video imagery in kenaf management and production. *Ind. Crops and Prod.* 9(3): 205-210.

Dabrowska-Zielinska, K., M. S. Moran, S. J. Maas, P. J. Pinter, Jr., B. A. Kimball, T. A. Mitchell, T. A. Clarke, and J. Qi. 2001. Demonstration of a remote sensing/modeling approach for irrigation scheduling and crop growth forecasting. *J. Water and Land Devel.* 5: 69-87.

Everitt, J. H., D. E. Escobar, R. Villarreal, J. R. Noriega, and M. R. Davis. 1991. Airborne video systems for agricultural assessment. *Remote Sensing of Environment* 35(2-3): 231-242, color plate p. 230.

Everitt, J. H., D. E. Escobar, K. R. Summy, and M. R. Davis, 1994. Using airborne video, global positioning system, and geographical information-system technologies for detecting and mapping citrus blackfly infestations. *Southwestern Entomologist* 19(2): 129-138.

Everitt, J. H., D. E. Escobar, K. R. Summy, M. A. Alaniz, and M. R. Davis. 1996. Using spatial information technologies for detecting and mapping whitefly and harvester ant infestations in south Texas. *Southwestern Entomologist* 21(4): 421-432.

Everitt, J. H., and M. R. Davis. 2004. Applications of airborne remote sensing in integrated pest management. *Subtropical Plant Science* 55 (1): 59-67.

Fletcher, R. S., and J. H. Everitt. 2007. A six-camera digital video imaging system sensitive to visible, red edge, near-infrared, and mid-infrared wavelengths. *Geocarto Intl.* 22(2): 75-86.

Franke, J., and G. Menz. 2007. Multi-temporal wheat disease detection by multi-spectral remote sensing. *Precision Agric.* 8(3): 161-172.

Gumz, M. S., and S. C. Weller. 2006. Differentiation of mint and weeds using spectral vegetation indices. *Proc. of the 8th Intl. Conf. on Precision Agric.* 8: 57. St. Paul, Minn.: Centre for Precision Agriculture.

Hart, W. G., and V. I. Myers. 1968. Infrared aerial color photography for detection of populations of brown soft scale in citrus groves. *J. Economic Entomology* 61(3): 617-624.

Hart, W. G., S. J. Ingle, M. R. Davis, and C. Mangum. 1973. Aerial photography with infrared color film as a method of surveying for citrus blackfly. *J. Economic Entomology* 66(1): 190-194.

Heald, C. M., W. J. Thames, and C. L. Wiegand. 1972. Detection of *Rotylenchulus reniformis* infestations by aerial infrared photography. *J. Nematology* 4: 298-300.

Henneberry, T. J., W. G. Hart, L. A. Bariola, D. L. Kittock, H. F. Arle, M. R. Davis, and S. J. Ingle. 1979. Parameters of cotton cultivation from infrared aerial photography. *Photogrammetric Eng. & Remote Sensing* 45(8): 1129-1133.

Hickman, M. V., J. H. Everitt, D. E. Escobar, and A. J. Richardson. 1991. Aerial-photography and videography for detecting and mapping Dicamba injury patterns. *Weed Tech.* 5(4): 700-706.

Jang, G. S., K. A. Sudduth, S. Y. Hong, N. R. Kitchen, and H. L. Palm. 2005. Relating image-derived vegetation indices to crop yield. In *Proc. 20th Biennial Workshop on Aerial Photography, Videography, and High Resolution Digital Imagery for Resource Assessment*, eds. C. Yang and J. H. Everitt. Bethesda, Md.: American Society for Photogrammetry and Remote Sensing.

Medlin, C. R., D. R. Shaw, P. D. Gerard, and F. E. LaMastus. 2000. Using remote sensing to detect weed infestation in *Glycine max.* *Weed Sci.* 48(3): 393-398.

Pinter, P. J., Jr. J. L. Hatfield, J. S. Schepers, E. M. Barnes, M. S. Moran, C. S. T. Daughtry, and D. R. Upchurch. 2003. Remote sensing for crop management. *Photogrammetric Eng. & Remote Sensing* 69(6): 647-664.

Qin, Z., M. Zhang, T. Christensen, T. W. Li, and H. Tang. 2003. Remote sensing analysis of rice disease stresses for farm pest management using wide-band airborne data. *Geoscience and Remote Sensing Symposium IGARSS. Proc. IEEE Intl.* (4): 2215-2217.

Richardson, A. J., R. M. Menges, and P. R. Nixon. 1985. Distinguishing weed from crop plants using video remote-sensing. *Photogrammetric Eng. & Remote Sensing.* 51(11): 1785-1790.

Schneider, C. L., and G. R. Safir. 1975. Infrared aerial photography estimation of yield potential in sugarbeets exposed to blackroot disease. *Plant Disease Reporter* 59(8): 627-631.

Thomson, S. J., P. V. Zimba, C. T. Bryson, and V. J. Alarcon-Calderon. 2005. Potential for remote sensing from agricultural aircraft using digital video. *Applied Eng. in Agric.* 21(3): 531-537.

Willers, J. L., J. N. Jenkins, W. L. Ladner, P. D. Gerard, D. L. Boykin, K. B. Hood, P. L. McKibben, S. A. Samson, and M. M. Bethel. 2005. Site-specific approaches to cotton insect control. Sampling and remote sensing analysis techniques. *Prec. Agric.* 6: 431-452.

Willis, P. R., P. G. Carter, and C. J. Johansen. 1998. Assessing yield parameters by remote sensing techniques. In *Proc. 4th Intl. Conf. on Precision Agric.*, eds. P. C. Robert, R. H. Rust, and W. E. Larson, 1465-1473. Madison, Wis.: ASA/CSSA/SSSA.

Yang, C., J. H. Everitt, J. N. Bradford, and D. E. Escobar. 2000. Mapping grain sorghum growth and yield variations using airborne multispectral digital imagery. *Trans. ASAE* 43(6): 1927-1938.

Yang, C., J. H. Everitt, and J. M. Bradford. 2002. Airborne hyperspectral imaging and yield monitoring of grain sorghum yield variability. ASAE Paper No. 021079. St. Joseph, Mich.: ASAE.

Yang, C., C. J. Fernandez, and J. H. Everitt. 2003. Mapping cotton root rot infestations with airborne multispectral imagery. ASAE Paper No. 031109. St. Joseph, Mich.: ASAE.



- Yang, C., J. H. Everitt, and J. M. Bradford. 2004. Airborne hyperspectral imagery and yield monitor data for estimating grain sorghum yield variability. *Trans. ASAE* 47(3): 915-924.
- Yang, C., C. J. Fernandez, and J. H. Everitt. 2005. Mapping phymatotrichum rot of cotton using airborne three-band digital imagery. *Trans. ASABE* 48(4): 1619-1629.
- Yang, C., J. H. Everitt, and J. M. Bradford. 2007. Comparison of airborne multispectral and hyperspectral imagery for yield estimation. ASABE Paper No. 071058. St. Joseph, Mich.: ASABE.
- Ye, X., K. Sakai, S. Asada, and A. Sasao. 2007. Use of airborne multispectral imagery to discriminate and map weed infestations in a citrus orchard. *Weed Biol. and Mgmt.* 7(1): 23-30.

